Electronic and crystal structure of NiTi martensite

Mahdi Sanati
Department of Physics, University of Cincinnati, Cincinnati, Ohio 45221
and Theoretical Division, Los Alamos National Laboratory, Los Alamos, New Mexico 87545

R. C. Albers
Theoretical Division, Los Alamos National Laboratory, Los Alamos, New Mexico 87545

F. J. Pinski
Department of Physics, University of Cincinnati, Cincinnati, Ohio 45221
(Received 27 February 1998)

All of the first-principles electronic-structure calculations for the martensitic structure of NiTi have used the experimental atomic parameters reported by Michal and Sinclair [Acta Crystallogr., Sect. B: Struct. Crystallogr. Cryst. Chem. **B37**, 1803 (1981)]. We have used first-principles, full-potential, linear muffin-tin orbital calculations to examine the total energy of all the experimental martensitic structures reported in the literature. We find that another crystal structure, that of Kudoh *et al.* [Acta Metall. Mater. **33**, 2049 (1985)], has the lowest total energy at zero temperature. Ground-state and formation energies were calculated for all of the experimental structures. Total and local densities of states were calculated and compared with each other for the structures of both Kudoh *et al.* and Michal and Sinclair [S0163-1829(98)01636-1]

I. INTRODUCTION

The $B2$ (bcc-like CsCl structure) phase of NiTi, also called nitinol, has been used for more than three decades as a shape memory alloy for couplings, fastener, connectors, and actuators in the automotive and aerospace industries, and for electronics, mechanical engineering, and medical applications. This material transforms martensitically from the parent $B2$ phase to a monoclinic martensitic phase with an intermediate orthorhombic R phase, from which a reversible shape memory effect—with the best shape memory behavior of all shape-memory alloys—and pseudoelasticity results. To understand the martensitic transformation, it is essential to know the crystal structure of the martensitic and parent phases as precisely as possible. However, the nitinol martensitic crystal structure has been controversial for a long time.[1] One reason for this has been the lack of single-crystal diffraction measurements for precise crystal-structure analysis, because single crystals of the alloys were very difficult to obtain in the martensitic phase. Since 1971, all investigators have agreed that the parent phase in nitinol is a CsCl-type structure, known as $B2$, and that the martensite phase is monoclinic, known as $B19'$. Nonetheless, although there is agreement on the overall unit cell between different experiments, the positions of the atoms within the unit cell differ considerably (Tables I and II). Historically, in 1971, Otsuka *et al.*[2] identified the martensitic structure in nitinol as a monoclinic structure of $P2/c$ symmetry. In the same year, however, Hehemann and Sandrock[3] (HS) noted that in some of the martensitic variants of their nitinol sample, the unit cell is monoclinic with $P2_1/m$ symmetry, with atomic coordinates that have slightly smaller bond lengths between the Ti and Ni atoms in the cell. Continuing this study, in 1981 Michal and Sinclair[4] (MS) concluded that the martensite is a monoclinic $P2_1/m$-type structure, but with some small differences in the coordinates of atoms as compared with those given in Ref. 2. In an attempt to obtain more accurate data, in 1983 Bührer *et al.*[5] (BGKMS) used a power-type nitinol specimen in a neutron-diffraction experiment. They concluded that the martensite in nitinol is monoclinic of the type $P2_1/m$, which is slightly more distorted and slender than the unit cells proposed in Refs. 2–4. Finally, in 1985 Kudoh *et al.*[6] (KTMO) analyzed the structure in a straightforward manner by utilizing a x-ray four-circle diffractometer. They concluded that the martensite unit cell is of the type $P2_1/m$.

Although theoretical calculations of equilibrium volume and lattice constants are straightforward calculations in first-principles electronic-structure methods, because of their smaller energy differences, it is much more difficult to compute small changes of the atomic positions inside the unit cell. These parameters are therefore usually based on experimental measurements. In this respect, NiTi poses an interesting problem, since three different values for the atomic positions have been reported (Fig. 1). Although experimentalists[7–9] tend to favor the KTMO crystal structure, because of the better accuracy of the experimental fit to the data, all of the available first-principles band-structure calculations[10–15] of the monoclinic martensitic NiTi crystal

TABLE I. Comparisons of lattice parameters for NiTi martensite.

Experiment	HS	MS	BGKMS	KTMO
a(Å)	2.883	2.885	2.884	2.898
b(Å)	4.117	4.120	4.110	4.108
c(Å)	4.623	4.622	4.665	4.646
$\beta(^\circ)$	96.8	96.8	98.10	97.78
Atoms/unit cell	4	4	4	4
Space group	$P2_1/m$	$P2_1/m$	$P2_1/m$	$P2_1/m$

TABLE II. Comparisons of atomic positions (conventional coordinates) for NiTi martensite.

Experiment	Ti	Ni
HS	0, 0, 0 0, $\frac{1}{2}$, $\frac{5}{8}$	$\frac{1}{2}$, 0, $\frac{1}{2}$ $\frac{1}{2}$, $\frac{1}{2}$, $\frac{1}{8}$
MS	0, 0, 0 0.055, $\frac{1}{2}$, 0.558	0.580, 0, 0.472 0.475, $\frac{1}{2}$, 0.086
BGKMS	0, 0, 0 0.122, $\frac{1}{2}$, 0.534	0.595, 0, 0.437 0.527, $\frac{1}{2}$, 0.097
KTMO	0, 0, 0 0.1648, $\frac{1}{2}$, 0.5672	0.6196, 0, 0.4588 0.5452, $\frac{1}{2}$, 0.1084

structure have been based on the crystal structure reported by MS.[4] No reasons were given in any of the theoretical papers why the MS parameters were preferred to other published structures. For this reason, we have decided to do a more extensive set of theoretical calculations to see if an examination of total energies could determine the correct crystal structure.

In this paper, we report and compare calculations of the ground-state and formation energies of NiTi martensite for the different experimental atomic parameters. We show that the KTMO crystal structure has the lowest zero-temperature energy. We compare ground-state and formation energies for all of the different crystal structures, and show the differences in the total and local densities of states (DOS) between the MS and KTMO structures.

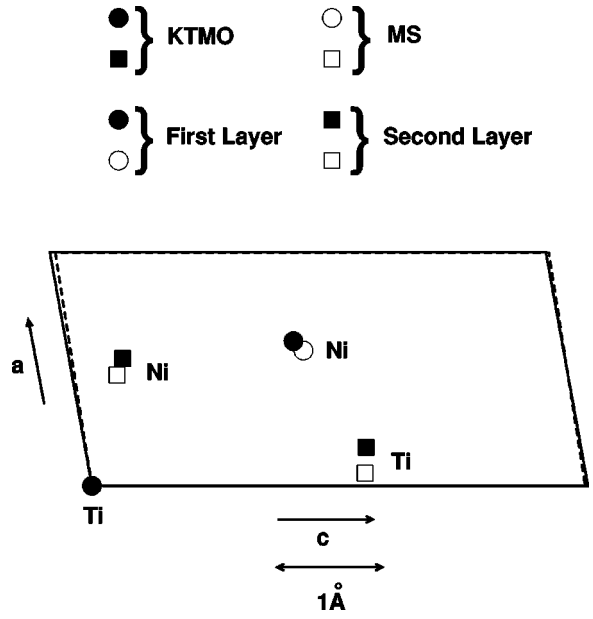

FIG. 1. The crystal structure of Ni-Ti martensite for the KTMO (solid line) and the MS (dashed line) structure, viewed from the [010] direction. The atom configurations in the conventional unit cell are shown. Filled and open symbols are the KTMO and MS atomic positions, respectively.

TABLE III. Ground-state and formation energies for NiTi martensite. The ground-state energy is relative to the $B2$ structure, which is $-2375.331\,62$ Ry/atom ($-32\,318.044\,91$ eV/atom).

Experiment	Ground-state energy mRy/atom (meV/atom)	Formation energy kJ/atom
$B2$	0. (0.)	−38.00
HS	6.90 (93.88)	−28.95
MS	−0.79 (−10.75)	−39.04
BGKMS	−2.34 (−31.84)	−41.07
KTMO	−3.41 (−46.39)	−42.48

II. CALCULATIONAL DETAILS AND DISCUSSION

In our calculations we have used a full-potential linear muffin-tin orbital technique.[16–18] The calculations were all electron, fully relativistic (with the spin-orbit coupling included at each variational step[19,20]), and employed no shape approximation to the charge density or potential. The base geometry was nonoverlapping muffin-tin spheres; the basis function, charge density and potential were expanded in spherical harmonics within the muffin-tins and in Fourier series in the interstitial region. The basis set was comprised of augmented linear muffin-tin orbitals.[19,20] The tails of the basis functions (the extension of the basis functions outside their parent spheres) were either Hankel or Neuman functions with nonzero kinetic energy. Four different tail values of the kinetic energy were used in these calculations. Spherical harmonic expansions were carried out through $l=8$ for the basis functions, charge density, and potential. For sampling the irreducible wedge of the Brillouin zone, we used the special **k**-point method[21,22] with 260 and 220 **k** points for monoclinic ($B19'$) and bcc ($B2$) structures, respectively. To speed convergence of the ground-state energies we associated each calculated eigenvalue with a Gaussian function having a width of 5 mRy. The linearized tetrahedron method was used to calculate the total and local DOS. Finally, the calculations used the Hedin-Lundqvist exchange-correlation

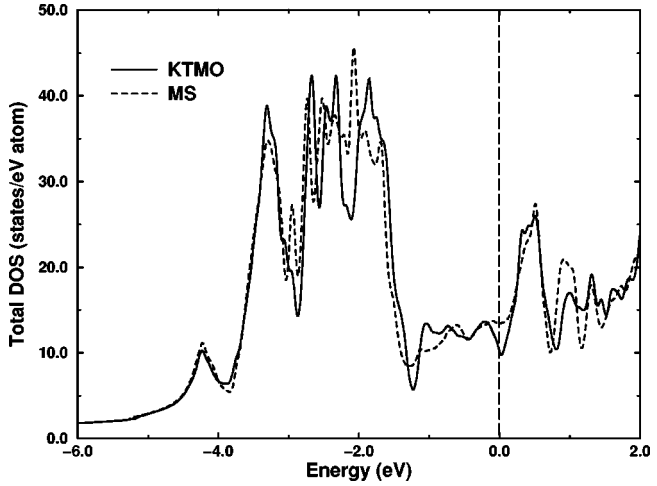

FIG. 2. Densities of states of NiTi martensite for the KTMO (solid line) and the MS (dashed line) experimental crystal structures.

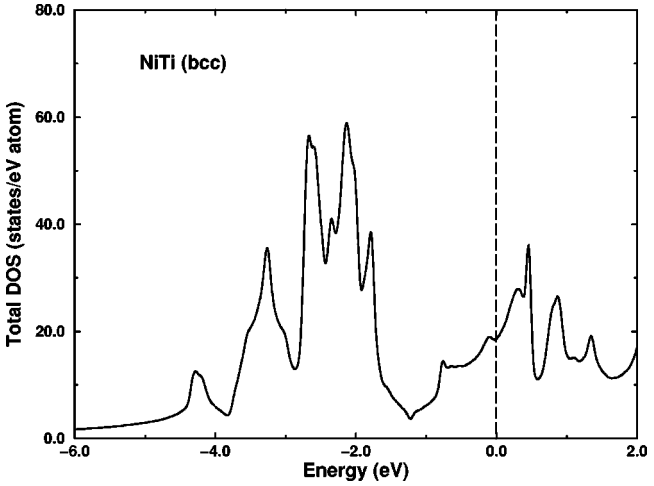

FIG. 3. Density of states for $B2$ NiTi.

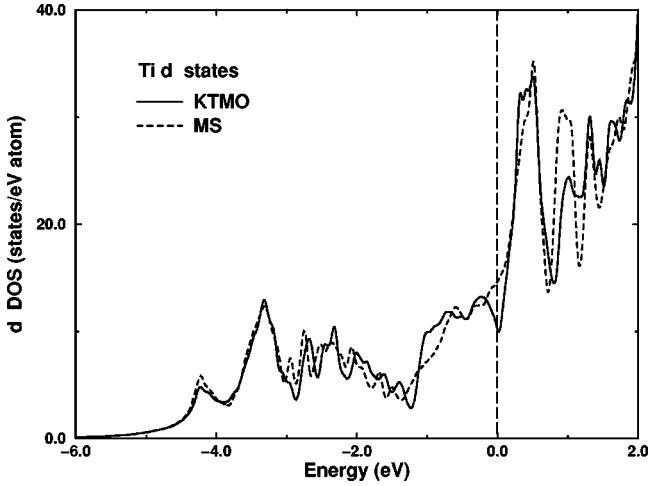

FIG. 5. Ti d-like densities of the states in NiTi martensite for the KTMO (solid line) and MS (dashed line) experimental crystal structures.

functional with gradient corrections to the exchange and correlation included.

The formation energies for different experiments were obtained by subtracting the weighted sum of the total energies of the constituent elements from the total energy of the compound, $\Delta E = E_{\mathrm{Ni}_a\mathrm{Ti}_b} - (aE^{fcc}_{\mathrm{Ni}} + bE^{hcp}_{\mathrm{Ti}})$.

Our results for the ground-state and formation energies showed significant differences between the different crystal structures, with the KTMO structure having the lowest ground-state energy (Table III). Our formation energy (-37.8 kJ/atom) for the MS experimental structure is in good agreement with the other reported first-principles values.[13] It is likely that the small difference between the two sets of calculations is because we used the experimental instead of the calculated equilibrium value for the lattice constant.

In principle, we could have tried to find the crystal structure that the local-density approximation calculations would predict based on a minimization of the total energy. However, because of the large number of parameters (12 in all) that would need to be optimized, we chose not to do this. With the high degree of accuracy required to converge the total energy to the required precision, such a large number of calculations would be very expensive computationally. We therefore restricted the scope of this paper to the experimental geometries.

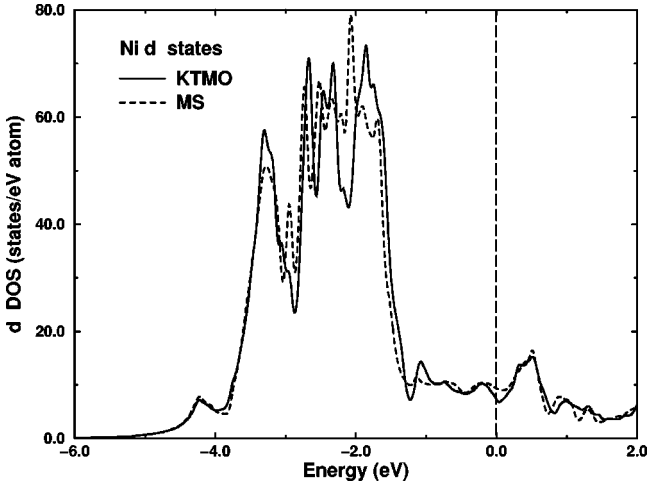

FIG. 4. Ni d-like densities of states in NiTi martensite for the KTMO (solid line) and the MS (dashed line) experimental crystal structures.

In addition to the total energy, we calculated the total DOS for both the KTMO and MS lattice parameters (Fig. 2), as well as for the bcc crystal structure (Fig. 3). The calculated total DOS for the MS atomic parameters is very similar to the other calculations[12,13] and is dominated by the Ni and Ti d-projected DOS (Figs. 4 and 5). While the overall placement and structure of the MS and KTMO bands are similar, their fine-scale features are different. In particular, the KTMO structure has a significantly lower DOS at the Fermi energy (cf. Fig. 2 and Table IV), which may partially explain its greater stability.

The x-ray photoelectron spectra (XPS) experiments[23,24] showed that the forms of spectra do not significantly change at the martensitic transformation and display fine structure in both parent and martensite states. If we compare the total and d-projected densities of states of these structures with the bcc structure, we note that on a broad scale they are remarkably similar. With the inherent significant instrumental and excited state broadening in an XPS experiment, it is not surprising that the XPS should be somewhat similar.

Selected interatomic distances for the Ti-Ni bond are

TABLE IV. Total and projected DOS for NiTi martensite at the Fermi energy (in states/eV atom).

Experiment	MS	KTMO
TDOS	13.35	10.15
Ti		
s	0.21	0.14
p	0.93	1.06
d	14.59	10.1
Ni		
s	0.34	0.32
p	1.22	1.34
d	9.26	7.22

TABLE V. Selected interatomic distances (Å) for NiTi. The bond-length variation is the difference between the longest and shortest bonds in the cluster of seven nearest-neighbor bonds for the martensitic structures.

Experiment	HS	MS	BGKMS	KTMO
Martensite ($B19'$)				
Ti-Ni	2.541×2	2.480×2	2.473×2	2.528×2
	2.570×2	2.587×1	2.488×1	2.529×1
	2.618×2	2.593×1	2.542×1	2.594×1
	2.865×2	2.615×2	2.558×2	2.599×2
		2.618×1	2.720×1	2.605×1
		3.118×1	3.334×1	3.282×1
Bond-length variation	0.324	0.138	0.247	0.077
Austenite ($B2$)				
Ti-Ni	2.611×8			

given in Table V. The lines in the table separate the bond lengths which are bigger or smaller than the $B2$ Ni-Ti bonds (last line of the table). The monoclinic $B19'$ structure has seven short Ti-Ni bonds instead of the eight for the bcc structure. These seven most closely resemble the $B2$ lattice for the KTMO structure. Also, the range of Ti-Ni bond lengths is greatly reduced relative to other published structures (c.f. the bond-length variation). This may make it easier for the martensitic transformation to occur.

III. CONCLUSION

In conclusion, we showed that the KTMO experimental parameters give the lowest zero-temperature energy, in contrast to the MS parameters that have been used in all theoretical band-structure calculations. This would tend to confirm the arguments of KTMO that their structure is the correct martensitic crystal structure, since their fit to the experimental x-ray diffraction patterns was significantly better. We would suggest that future electronic-structure calculations should use the KTMO crystal structure.

ACKNOWLEDGMENTS

This work was supported in part by the U.S. NSF and the U.S. DOE. M.S. and F.J.P. acknowledge financial support for this work from NSF Grant No. DMR95-31223.

[1] T. Tadaki and K. Shimizu, Mem. Inst. Sci. Ind. Res., Osaka Univ. **41**, 37 (1984).
[2] K. Otsuka, T. Sawamura, and K. Shimizu, Phys. Status Solidi A **5**, 457 (1971).
[3] R. F. Hehemann and G. D. Sandrock, Scr. Metall. **5**, 801 (1971).
[4] G. M. Michal and R. Sinclair, Acta Crystallogr., Sect. B: Struct. Crystallogr. Cryst. Chem. **B37**, 1803 (1981).
[5] W. Bührer, R. Gotthardt, A. Kulik, and F. Staub, J. Phys. F **13**, L77 (1983).
[6] Y. Kudoh, M. Tokonami, S. Miyazaki, and K. Otsuka, Acta Metall. Mater. **33**, 2049 (1985).
[7] W. Bührer, M. Zolliker, and R. Gotthardt, Scr. Metall. Mater. **26**, 1149 (1992).
[8] K. Otsuka and T. Ohba, ICOMAT-92, 221 (1993).
[9] K. Shimizu and T. Tadaki, Mater. Trans., JIM **33**, 165 (1992).
[10] S. E. Kulkova, V. E. Egorushkin, and V. V. Kalchikhin, Solid State Commun. **77**, 667 (1991).
[11] G. Bihlmayer, R. Eibler, and A. Neckel, J. Phys.: Condens. Matter **5**, 5083 (1993).
[12] S. E. Kulkova, K. A. Beketov, V. E. Egorushkin, and O. N. Muryzhnikova, J. Phys. IV **5**, 539 (1996).
[13] A. Pasturel, C. Colinet, D. Nguyen Manh, A. T. Paxton, and M. van Schilfgaarde, Phys. Rev. B **52**, 15 176 (1995).
[14] G. Bihlmayer, R. Eibler, and A. Neckel, Philos. Mag. B **73**, 511 (1996).
[15] J. M. Zhang and G. Y. Guo, Phys. Rev. Lett. **78**, 4789 (1997).
[16] J. M. Wills (unpublished).
[17] J. M. Wills and B. R. Cooper, Phys. Rev. B **36**, 3809 (1987).
[18] D. L. Price and B. R. Cooper, Phys. Rev. B **39**, 4945 (1989).
[19] O. K. Andersen, Phys. Rev. B **12**, 3060 (1975).
[20] H. L. Skriver, *The LMTO Method* (Springer-Verlag, Berlin, 1984).
[21] D. J. Chadi and M. L. Cohen, Phys. Rev. B **8**, 5747 (1973).
[22] S. Froyen, Phys. Rev. B **39**, 3168 (1989).
[23] S. A. Shabalovskaja, A. I. Lotokov, I. I. Sasovskaja, A. G. Narmonev, and A. I. Zakharov, Solid State Commun. **32**, 735 (1979).
[24] S. Shabalovskaya, A. Narmonev, O. Ivanova, and A. Dementjev, Phys. Rev. B **48**, 13 296 (1993).